Analysis of the Impact of Relative Humidity and Mineral Coarse Mode Aerosols Particle Concentration on the Visibility and particle size distribution of Desert Aerosols

Yerima S. U[1], Abdulkarim U. Y[2], Tijjani B. I[3], Gana U. M[4], Sani M[5], Aliyu R[6], Shamsuddeen M. F[7],Khamisu U.Y[8] and Abdulhadi D[9]

Abstract –This paper presents the results of the Analysis of the Impact of relative humidity and Mineral Coarse Mode Aerosols Particle Concentration on the visibility and particle size distribution of desert aerosols based on microphysical properties of desert aerosols. The microphysical properties (the extinction coefficients, volume mix ratios, dry mode radii and wet mode radii) were extracted from Optical Properties of Aerosols and Clouds (OPAC 4.0) at eight relative humidities (00 to 99%RH) and at the spectral range of 0.4-0.8 μm. the concentrations of mineral coarse component (MINC) were varied to obtain five different models. The angstrom exponent (α), the turbidity (β), the curvature (α_2), humidification factor (γ), the mean exponent of aerosol growth curve (μ) and the mean exponent of aerosol size distributions (v) were determined from the regression analysis of some standard equations. It was observed that the values of (α) are less than 1 throughout the five models which signifies the dominance of coarse mode particles over fine mode particles. It was observed that the curvature (α_2) has both monomodal and bimodal types of distributions all through the five models and this signifies the dominance of coarse mode particles with some traces of fine mode particles. The visibility was observed to decrease with the increase in RH and increased with wavelength. The analysis further found that there is an inverse power law relationship between humidification factor, the mean exponent of the aerosol size distribution with the mean exponent of the aerosol growth curve (as the magnitude of (μ) decreases across the five models, the magnitudes of (γ) and (v) increase, but the magnitude of both (γ) and (v) increases for a given (μ) across the individual models). The mean exponent of aerosol size distribution (μ) being less than 3 indicate hazy condition of the desert atmosphere.

Keywords– Extinction coefficient, Visibility Enhancement parameter, mean exponent of the aerosol size distribution, humidification factor, mean exponent of the aerosol growth curve.

[1] Nigerian Meteorological Agency (NIMET), Nnamdi Azikwe International Airport Abuja. sunusiyerima@yahoo.com, sunusiyerima86@gmail.com +234 8037335747
[2] Department of Physics, Saadatu Rimi Collage of Education Kano, Kano State, Nigeria.
[3] Department of Physics, Bayero University Kano, Kano State, Nigeria.
[4] Department of Physics, Bayero University Kano, Kano State, Nigeria.
[5] Center for Atmospheric Research, National Space Research and Development Agency (NARSDA), Anyigba, Nigeria.
[6] Department of Physics, Kano State University of Science and Technology Wudil, Kano State, Nigeria.
[7]Department of Physics, Faculty of science Federal University Dutse, Jigawa State Nigeria.
[8]Remedial and General Studies Department, Audu Bako Collage of Agriculture Danbatta, kano, Kano State, Nigeria.

1 INTRODUCTION

Propagation of mineral dust, electromagnetic radiation at infrared frequencies through the atmosphere is affected by absorption and scattering caused mostly by particulate matter (haze. dust, fog, and cloud droplets) suspended in the air [1]. Scattering and absorption by haze particles or aerosols becomes the dominant factor in the boundary layer near the earth's surface, especially under low visibility conditions [2]. Mineral dust particles in the atmosphere vary greatly in their size, concentration, formation, and also in their impact on climate at regional or global scale [3].

Visibility is one of the most important parameter in the study of climate and air quality; it is one of the most efficient way to study the level of air pollution in the world [4]. visibility in climate study is defined as maximum distance at which a dark object can be seen against a light sky [5]. also, visibility is defined as the greatest horizontal distance at which a large object can be seen and recognized against its surrounding [6]. Change in visibility is related to significant scattering and absorption of solar radiation by suspended particles in the atmosphere [7]. The mineral coarse mode particles are emitted by both natural and anthropogenic sources such as dust storm, biomass burning, digging of soil through farming and irrigation, forest fire, vegetation, secondary inorganic salts, sea spray and the rising harmattan dust [8]. The aerosols produce may include mineral dust, smoke, organic matter, gas pollutant and airborne particles at different quantity in the atmosphere. Visibility can also be influenced by meteorological conditions such the relative humidity of an area.

It is well know that one of the most critical challenges facing desert atmospheric research has to do with understanding the intricate links between the highly variable climate patterns and the increasing atmospheric aerosol loading trends being reported in many parts of the world [4]. Varying concentrations and composition of atmospheric aerosol particles immensely influence the global climate system in a number of ways especially due to aerosol radiative and microphysical properties [6]. However, the potential impact of varying the mineral coarse mode aerosols concentrations and change in relative humidity on the visibility of the desert atmosphere have been understudied.

Mineral dust can greatly affect visibility, climate, biogeochemical processes, atmospheric process and possibly human health [9]. The magnitude of the impact of dust depends on particle size [7]. other studies [5], [9], [10], said that dust aerosol is recognized as the principle pollutant that causes low visibility in many parts of the world [11]. This is due to the position of the regions where dust aerosols are being transported regularly from Sahara desert [12].

In this paper the extinction coefficients, volume mix ratios, dry mode radii and wet mode radii of desert aerosols were extracted from OPAC (4.0) at the spectral wavelength of 0.4 to 0.8μm, and at relative humidities of 0, 50, 70, 80, 90, 95, 98 and 99%. From the four components of the aerosols, (WASO, MINN, MIAN MICN) the mineral (coarse mode, nonspherical) MICN was varied. The parameters were analyzed using excel, SPSS, Origin and some standard formulae and determined the effective hygroscopic growth, humidification factor, visibility enhancement parameter, visibility, the mean exponent of aerosol growth curve and the mean exponent of aerosol size distribution.

2 METHODOLOGY

The table 1 shows the models components of the compositions of the desert aerosols used to determine the extinction coefficients of the mixture.

Table1: The models used in the simulations of the desert aerosols.

	Model1	Model2	Model3	Modle4	Model5
Comp	No. Den. (cm^{-3})	No. Den. (cm^{-3})	No. Den. (cm^{-3})	No. Den. (cm^{-3})	No. Den. (cm^{-3})
WASO	2000	2000	2000	2000	2000
MINN	289.5	309.5	329.5	349.5	369.5
MIAN	30.5	30.5	30.5	30.5	30.5
MICN	0.142	0.142	0.142	0.142	0.142

An objective measure of visibility is the standard visual range or meteorological range [13].

$$Vis(\lambda) = \frac{3.912}{\sigma_{ext}(\lambda)} \quad (1)$$

Meteorological range refers to the visual range of a black object seen against its surrounding [14]. The visual extinction coefficient $\sigma_{ext}(\lambda)$ is the measure of light scattering and absorbing properties of the atmosphere along the line of sight [15]. To determine the visibility using the extracted extinction coefficient, the variation of the extinction coefficient with wavelength was determined using the inverse power law of extinction coefficient as;

$$\sigma_{ext}(\lambda) = \beta\lambda^{-\alpha} \quad (2)$$

where α and β are known as Angstrom parameters. The index α is the wavelength exponent or Angstrom coefficient and β is the turbidity coefficient representing the amount of aerosols present in the atmosphere in the vertical direction or the total aerosol loading in the atmosphere [13,14].

Substituting equation (2) into (1), the following equation is obtained which is the variation of the visibility with wavelength.

$$Vis(\lambda) = \frac{3.912}{\beta}\lambda^{\alpha} \quad (3)$$

Equation (3) can also be written as

$$ln\left(\frac{Vis_{\lambda}}{3.912}\right) = -ln(\beta) + \alpha\, ln(\lambda) \quad (4)$$

To obtain α (slope) and β (intercept) a regression analysis was performed using an expression derived from the Kaufman (1993) representation of the equation [18].

However, The Angstrom exponent itself varies with wavelength, and a more precise empirical relationship between visibility and wavelength is obtained with a 2nd-order polynomial [9,16,19]

$$ln\left(\frac{Vis_{\lambda}}{3.912}\right) = -ln(\beta) + \alpha_1 ln(\lambda) + \alpha_2\left(ln(\lambda)\right)^2 \quad (5)$$

Here, the coefficient α^2 accounts for a "curvature" often observed in the sun photometry measurements. Some authors have noted that the curvature is also an indicator of the aerosol particle size, with negative curvature indicating aerosol size distributions dominated by the fine mode and positive curvature indicating size distributions with a significant coarse mode contribution [20,23].

Now, to determine the relationship between visibility and relative humidity, enhancement parameter is defined as [28].

$$f(RH,\lambda) = \frac{Vis(RH,\lambda)}{Vis(RH=0,\lambda)} = \left[\frac{1-(RH)}{1-(RH=0)}\right]^{-\gamma} \quad (6)$$

Now taking the natural log of both side we have

$$ln\left(\frac{Vis(RH,\lambda)}{Vis(0,\lambda)}\right) = -\gamma ln(1-RH) \quad (7)$$

Also, γ is given as (Tijjani, 2013)

$$\gamma = \frac{(\upsilon-1)}{\mu} \quad (8)$$

Where γ is the humidification factor representing the dependence of visibility on RH, It arises from the change in the particle size and refractive indices upon humidification [9,24]. The use of γ has an advantage of describing the hygroscopic behavior of visibility in a linear manner over a broad range of RH values, and also implies that particles are deliquesced [30], the γ parameter is dimensionless, and it increases with increase in particle water uptake [9]. μ is defined as the mean exponent of the aerosol growth curve constant, υ as the mean exponent of the aerosol size distribution [28].

Junge, (1958) have demonstrated the need for using logarithmic range for the interpretation of the mean exponent of the aerosol size distributions [31]. Based on experimental observations, he proposed a power law size distribution function of the form;

$$\frac{dn(r)}{d(logr)} = Cr^{-\upsilon} \quad (9)$$

Where dn(r) is the number of particles with radii between r and r+dr, C is constant depending on the number of particles in one cubic centimeter and the exponent υ determines the mean exponent of aerosol size distribution. As υ values decrease the number of larger particles increases compared to smaller particles [24].

Now, the hygroscopic growth g(RH) experienced by a single aerosol particle according to [28] is given by

$$g(RH) = \frac{r(RH)}{r(RH=0)} \quad (10)$$

where r(RH) is the radius at RH% and r(RH=o) is the radius at 0%RH.

Now, the effective hygroscopic growth of the four components of the aerosols is given as:

$$g_{eff}(RH) = \left(\sum_i x_i g_i^3(RH)\right)^{\frac{1}{3}} \quad (11)$$

where the summation is performed over all compounds present in the particles and x_i represents the respective volume fraction of single aerosol particle concentration and g_i is the hygroscopic growth of the i^{th} aerosol particles using the Zdanovskii-Stokes-Robinson relation [32], and i= 1,2,3,4.

Now, expressing the effective hygroscopic growth in terms of relative humidity we have:

$$g_{eff}(RH) = \left[\frac{1-(RH)}{1-(RH=0)}\right]^{-\frac{1}{\mu}} \quad (12)$$

where μ is defined as the mean exponent of the aerosol growth curve constant as defined in equation (8)

taking the natural log of both side we have:

$$\ln g_{eff}(RH) = -\frac{1}{\mu}\ln(1-RH) \quad (13)$$

Now, expressing υ (the mean exponent of the aerosol size distribution) in terms of μ and γ (the humidification factor) using equations (8) and (12) we have:

$$\upsilon = \gamma\mu + 1 \quad (14)$$

3 Results and Discussion

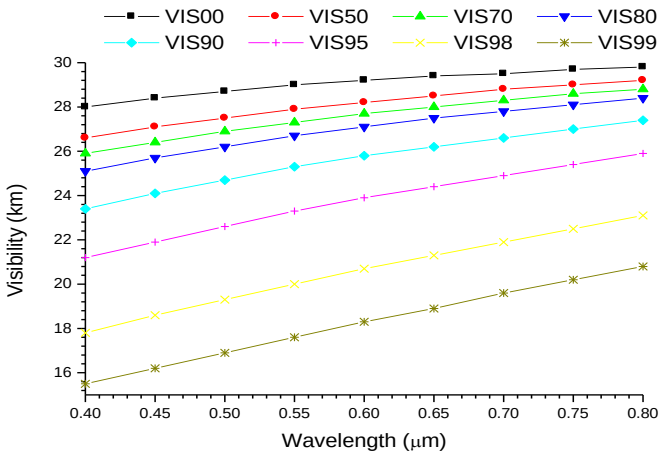

Figure 1 a graph of visibility against wavelength for micn model 1

From fig. 1, it can be observed that the visibility increased with the increase in wavelength, and decreases with the increase in relative humidity (RH). It can also be observed that the visibility is lower at shorter wavelengths with maximum and minimum values of 28.1km and 15.89km respectively. This shows the dominance of coarse mode particles with some traces of fine mode particles. It should also be noted that fine mode particles scatter and absorb more solar radiation than the coarse mode particles [33]. Since from equation (3) the visibility is the inverse of extinction, this implies that the visibility will be lower at shorter wavelengths. The change in visibility is more pronounced from 80%RH to 99%RH and at higher wavelengths.

Table 2 Results of the regression analysis of equations (4) and (5) for visibility using SPSS.

	Linear			Quadratic			
RH	R^2	α	β	R^2	α_1	α_2	β
0%	0.9852	0.0920	0.1281	0.9891	0.0590	-0.0292	0.1291
50%	0.9834	0.1296	0.1297	0.9928	0.0573	-0.0641	0.1319
70%	0.9965	0.1580	0.1304	0.9978	0.1259	-0.0285	0.1314
80%	0.9935	0.1760	0.1322	0.9972	0.1146	-0.0545	0.1342
90%	0.9953	0.2262	0.1353	0.9963	0.1848	-0.0367	0.1367
95%	0.9991	0.2916	0.1416	0.9991	0.2944	0.0025	0.1415
98%	0.9988	0.3655	0.1567	0.9988	0.3647	-0.0007	0.1567
99%	0.9976	0.4260	0.1718	0.9993	0.5265	0.0891	0.1678

By observing the R^2 values from both the linear and quadratic part of Table 2, it can be seen that the data fitted the equation models very well. From the linear part, since α is less than 1, this signifies the dominance of coarse mode particles over fine mode particles. The increase of α with RH shows that coarse mode particles are being reduced from the atmosphere more than fine mode particles due to coagulation and sedimentation. Considering the quadratic part, it can be seen that α^2 is negative from 00% to 98%RH, and this shows monomodal distribution of coarse mode particles with very large traces of fine mode particles. It can also be observed from the quadratic part that α^2 is positive at 99%RH, which signifies bimodal type of distribution with coarse mode particles as dominance over coarse mode particles. The fluctuation in the magnitude of α^2 with RH shows the non-linearity relation between particles size distribution, RH and also with the physically mixed aerosols. the increase in turbidity coefficient β with RH also signifies decrease in visibility with increase in RH.

Table 3 the result of the analysis of equations (7), (13) and (14) using SPSS

	μ	12.7709	
λ	R^2	γ	υ
0.55	0.952257	0.089078	2.137606
0.65	0.943115	0.077094	1.98456
0.75	0.93441	0.066759	1.852573

By observing the values of R^2, it can be said that the data fitted the equation models very well. Equation (6) shows that the visibility satisfies the inverse power law with (1-RH). The decrease of humidification factor with the increase in wavelength also shows that the visibility increases with the increase in wavelength. Equation (12) shows that the hygroscopic growth has also satisfied the inverse power relation with (1-RH) and the reciprocal of mean exponent of aerosol growth curve. It can also be said that for a fixed value of mean exponent of the aerosol growth curve μ, the humidification factor γ decreases with the increase in wavelength, this also shows that the visibility increases with the increase in wavelength (as the particles size decreases) i.e it satisfies the inverse power law

of equation (6) and decreases with an increase in RH. Based on equation (9). the mean exponent of the aerosol size distribution (v) also decrease with the increase in wavelength which shows that the number of larger particles increase compared to smaller particles and this is due to major coagulation amount caused by the increase in number of fine mode particles and consequently the tiny particles coagulate more than the larger particles as said by (Junge 1958) and [34]. It can also be noted from the values of (v) that the average atmospheric condition of the area is foggy [31].

Table 4 the results of the analysis of skewness and kurtosis using SPSS.

	lnvis00	lnvis50	lnvis70	lnvis80	lnvis90	lnvis95	lnvis98	lnvis99
Skewness	-0.4655	-0.6001	-0.4274	-0.4992	-0.4124	-0.3080	-0.3125	-0.1851
Kurtosis	-1.1852	-0.8556	-0.9375	-1.0373	-0.8996	-1.1393	-1.1272	-1.2648

From Table 4, the behaviors and changes of particles size distribution are displayed in terms of vertical behavior (kurtosis) and horizontal behavior (skewness). From skewness, it can be seen that it is negative all through, this implies that it is negatively skewed and this signifies that the particle distribution is dominated by coarse mode particles. From the kurtosis, it can be observed that it is also negative all through. Which signifies that it is platykurtic, and the average vertical size distribution of the particles is below normal size distribution. The fluctuations in the values of the values of skewness and kurtosis maybe due to the nonlinear relation between the particles size distribution with RH and the physically mixed aerosols.

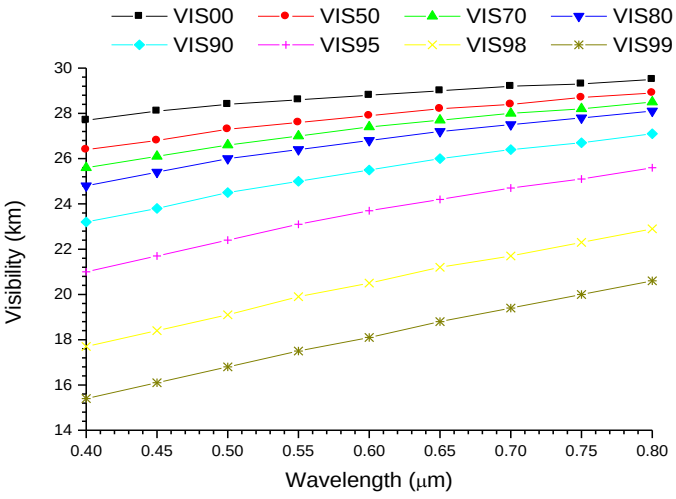

Figure 2 plot of visibility against wavelength for micn model 2

From figure 2, it can be observed that the visibility increases with the increase in wavelength, and decreases with the increase in relative humidity (RH). It can also be observed that the visibility is lower at shorter wavelengths with maximum and minimum values of 27.9km and 16.89km respectively. This shows the dominance of coarse mode particles with some traces of fine mode particles. It should also be noted that fine mode particles scatter and absorb more solar radiation than the coarse mode particles [33]. Since from equation (3) the visibility is the inverse of extinction, this implies that the visibility will be lower at shorter wavelengths. The change in visibility is more pronounced from 90%RH to 99%RH.

Table 5 Results of the regression analysis of equations (4) and (5) for visibility using SPSS.

	Linear			Quadratic			
RH	R^2	α	β	R^2	α_1	α_2	β
0%	0.983543	0.084078	0.130247	0.987011	0.055593	-0.02526	0.13113
50%	0.984782	0.126974	0.131460	0.987153	0.091422	-0.03153	0.132573
70%	0.996531	0.158017	0.131759	0.997796	0.125891	-0.02849	0.132767
80%	0.993475	0.176046	0.133575	0.997192	0.114604	-0.05449	0.135537
90%	0.995262	0.226201	0.136705	0.996284	0.184835	-0.03669	0.138053
95%	0.998324	0.288038	0.143111	0.998457	0.269081	-0.01681	0.143757
98%	0.998805	0.365523	0.158283	0.998806	0.364712	-0.00072	0.158313
99%	0.999067	0.415137	0.173981	0.999513	0.465208	0.044407	0.171926

By observing the R^2 values from both the linear and quadratic part of Table 5, it can be seen that the data fitted the equation models very well. From the linear part, since α (angstrom exponent) is less than 1, this signifies the dominance of coarse mode particles. The increase of α with RH shows that coarse mode particles are being reduced from the atmosphere more than fine mode particles due to coagulation and sedimentation. Considering the quadratic part, it can be seen that α^2 is negative from RH of 0 to 98%, and this shows monomodal distribution of coarse mode particles. But it changed to positive at 99%RH which signifies that it is bimodal type of distribution with coarse mode particles as dominant and traces of fine mode particles. The fluctuations of the magnitudes of α^2 with RH shows the non-linearity relation between particles size distribution, RH and also with the physically mixed aerosols. The increase in turbidity coefficient β with RH signifies decrease in visibility with increase in RH.

Table 6 the result of the analysis of equations (8) and (12) using SPSS.

	u	12.95236	
λ	R^2	γ	v
0.55	0.951782	0.088183	2.142178
0.65	0.942524	0.076226	1.987307
0.75	0.934189	0.066063	1.855672

By observing the values of R^2, it can be said that the data fitted the equation models very well. Equation (6) shows that the visibility satisfies the inverse power law with (1-RH). The decrease of humidification factor with wavelength also shows that the visibility increases with the increase in wavelength. Equation (12) shows that the hygroscopic growth has satisfied the inverse power relation also with (1-

RH) and the reciprocal of mean exponent of aerosol growth curve. It can also be said that for a fixed value of mean exponent of the aerosol growth curve μ, the humidification factor γ decreases with the increase in wavelength, this also shows that the visibility increases with the increase in wavelength (as the particles size decreases) i.e it satisfies the inverse power law of equation (6) and decreases with an increase in RH. Based on equation (9), the mean exponent of the aerosol size distribution (v) decrease with wavelength which shows that the number of larger particles increase compared to smaller particles and this is due to major coagulation amount caused by the increase in number of fine mode particles and consequently the tiny particles coagulate more than the larger particles as said by [29,32]. It can also be noted from the values of (v) that the average atmospheric condition of the area is foggy [31].

Table 7 the results of the analysis of skewness and kurtosis using SPSS.

	lnvis00	lnvis50	lnvis70	lnvis80	lnvis90	lnvis95	lnvis98	lnvis99
Skewness	-0.4688	-0.4518	-0.4274	-0.4992	-0.4124	-0.3526	-0.3125	-0.2434
Kurtosis	-0.8437	-0.9512	-0.9375	-1.0373	-0.8996	-0.9803	-1.1272	-1.0411

From Table 4, the behaviors and changes of particles size distribution are displayed in terms of vertical behavior (kurtosis) and horizontal behavior (skewness). From skewness, it can be seen that it is negative all through, this implies that it is negatively skewed and this signifies that the particle distribution is dominated by coarse mode particles. From the kurtosis, it can be observed that it is also negative all through, and this shows that it is platykurtic, and the average vertical size distribution of the particles is below normal size distribution. The fluctuations in the values of the values of skewness and kurtosis maybe due to the nonlinear relation between the particles size distribution with RH and the physically mixed aerosols.

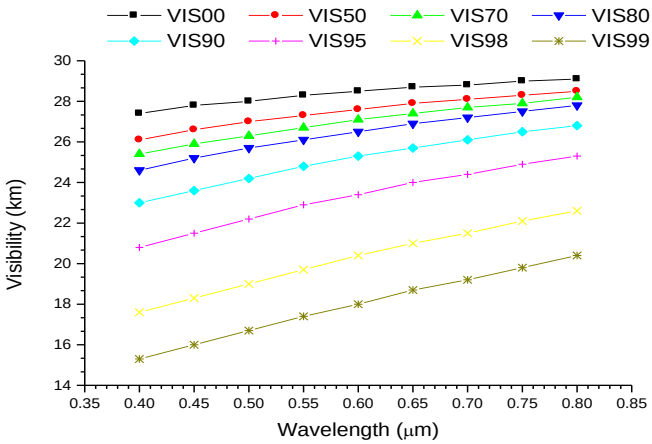

Figure 3 a graph of visibility against wavelength for micn model 3

From figure 3, it can be observed that the visibility increases with the increase in wavelength, and decreases with the increase in relative humidity (RH). It can also be observed that the visibility is lower at shorter wavelengths with maximum and minimum values of 26.5km and 14.3km respectively. This shows the dominance of coarse mode particles with some traces of fine mode particles. It should also be noted that fine mode particles scatter and absorb more solar radiation than the coarse mode particles [33]. Since from equation (3) the visibility is the inverse of extinction, this implies that the visibility will be lower at shorter wavelengths. The change in visibility is more pronounced from 80%RH to 99%RH.

Table 8 Results of the regression analysis of equations (4) and (5) for visibility using SPSS.

	Linear			Quadratic			
RH	R^2	α_1	β	R^2	α_2	α_1	β
0%	0.9835	0.0841	0.1316	0.9870	0.0556	-0.0253	0.1324
50%	0.9952	0.1241	0.1333	0.9958	0.1405	-0.0146	0.1328
70%	0.9867	0.1510	0.1337	0.9942	0.0762	-0.0664	0.1361
80%	0.9969	0.1755	0.1351	0.9979	0.1449	-0.0272	0.1361
90%	0.9946	0.2186	0.1389	0.9964	0.1654	-0.0472	0.1407
95%	0.9983	0.2880	0.1445	0.9985	0.2691	-0.0168	0.1452
98%	0.9994	0.3751	0.1505	0.9994	0.3803	0.0046	0.1503
99%	0.9987	0.4071	0.1761	0.9996	0.4742	0.0595	0.1733

By observing the R^2 values from both the linear and quadratic part of Table 8, it can be seen that the data fitted the equation models very well. From the linear part, since α (angstrom exponent) is less than 1, this signifies the dominance of coarse mode particles over fine mode particles. The increase of α with RH shows that coarse mode particles are being reduced from the atmosphere more than fine mode particles as a result of the increase in RH due to coagulation and sedimentation. Considering the quadratic part, it can be seen that α^2 is negative from RH of 00 to 95%, and this shows monomodal distribution of coarse mode particles. But from the RH of 98% to 99% it changed to positive and this indicates bimodal type of distribution with coarse mode particles as dominant with some traces of fine mode particles. The fluctuations of the magnitudes of α^2 with RH shows the non-linearity relation between particles size distribution, RH and the physically mixed aerosols. The increase in turbidity coefficient β with RH signifies decrease in visibility with increase in RH.

Table 9 the result of the analysis of equations (8) and (12) using SPSS.

	μ	13.13008	
λ	R^2	γ	v
0.55	0.950996	0.087216	2.145153
0.65	0.94189	0.075413	1.990179
0.75	0.933913	0.065305	1.85746

By observing the values of R^2, it can be said that the data fitted the equation models very well. Equation (6) shows

that the visibility satisfies the inverse power law with (1-RH). The decrease of humidification factor with wavelength also shows that the visibility increases with the increase in wavelength. Equation (12) shows that the hygroscopic growth has satisfied the inverse power relation also with (1-RH) and the reciprocal of mean exponent of aerosol growth curve. It can also be said that for a fixed value of mean exponent of the aerosol growth curve μ, the humidification factor γ decreases with the increase in wavelength, this also shows that as the particles size decreases, the visibility increased with the increase in wavelength i.e it satisfies the inverse power law of equation (6). Based on equation (9), the mean exponent of the aerosol size distribution (v) decrease with the increase in wavelength, which shows that the number of larger particles increase compared to smaller particles and this is due to major coagulation amount caused by the increase in number of fine mode particles and consequently the tiny particles coagulate more than the larger particles as said by [29,32]. It can also be noted from the values of (v) that the average atmospheric condition of the area is foggy [31].

Table 10 the results of the analysis of skewness and kurtosis using SPSS.

	lnvis00	lnvis50	lnvis70	lnvis80	lnvis90	lnvis95	lnvis98	lnvis99
Skewness	-0.4688	-0.2418	-0.5551	-0.4062	-0.4445	-0.3526	-0.3040	-0.2217
Kurtosis	-0.8437	-0.7605	-0.9405	-1.0516	-0.9576	-0.9803	-1.0721	-1.1687

From Table 10, the behaviors and changes of particles size distribution are displayed in terms of vertical behavior (kurtosis) and horizontal behavior (skewness). From skewness, it can be seen that it is negative all through, this implies that it is negatively skewed and this signifies that the particle distribution is dominated by coarse mode particles. From the kurtosis, it can be observed that it is also negative all through, and this shows that it is platykurtic, and the average vertical size distribution of the particles is below normal size distribution. The fluctuations in the values of the values of skewness and kurtosis maybe due to the nonlinear relation between the particles size distribution with RH and the physically mixed aerosols.

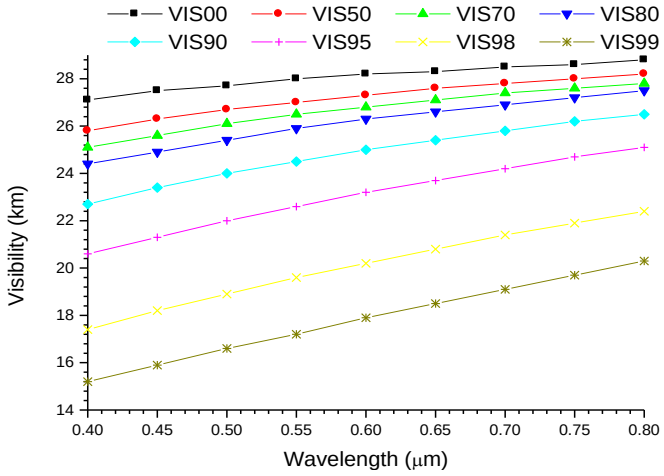

Figure 4 a graph of visibility against wavelength for micn model 4

From figure 4, it can be observed that the visibility increases with the increase in wavelength, and decreases with the increase in relative humidity (RH). It can also be observed that the visibility is lower at shorter wavelengths with maximum and minimum values of 27.4km and 15.5km respectively. This shows the dominance of coarse mode particles with some traces of fine mode particles. It should also be noted that fine mode particles scatter and absorb more solar radiation than the coarse mode particles [33]. Since from equation (3) the visibility is the inverse of extinction, this implies that the visibility will be lower at shorter wavelengths. The change in visibility is more pronounced from 90%RH to 99%RH.

Table 11 Results of the regression analysis of equations (4) and (5) for visibility using SPSS.

	Linear			Quadratic			
RH	R^2	α	β	R^2	α_1	α_2	β
0%	0.9846	0.0835	0.1331	0.9846	0.0859	0.0021	0.1330
50%	0.9952	0.1241	0.1346	0.9958	0.1405	0.0146	0.1341
70%	0.9853	0.1449	0.1358	0.9907	0.0539	0.0220	0.1311
80%	0.9969	0.1755	0.1365	0.9979	0.1449	-0.0272	0.1375
90%	0.9923	0.2192	0.1401	0.9968	0.1351	-0.0746	0.1430
95%	0.9978	0.2807	0.1463	0.9987	0.2332	-0.0422	0.1479
98%	0.9984	0.3606	0.1610	0.9991	0.4169	0.0499	0.1589
99%	0.9975	0.4167	0.1766	0.9986	0.4956	0.0700	0.1733

By observing the R^2 values from both the linear and quadratic part of Table 11, it can be seen that the data fitted the equation models very well. From the linear part, since α (angstrom exponent) is less than 1, this signifies the dominance of coarse mode particles with some traces of fine mode particles. The increase of α with RH shows that coarse mode particles are being reduced from the atmosphere more than fine mode particles as a result of the increase in RH due to coagulation and sedimentation. Considering the quadratic part, it can be seen that α^2 is negative from RH of 80 to 95%, and this shows monomodal distribution of coarse mode particles. It can also be observed that α^2 is positive from the RH of 00% to 70% and

98 to 99%RH which signifies bimodal type of distribution with coarse mode particles as dominant with some traces of fine mode particles. The fluctuations of the magnitudes of α^2 with RH shows the non-linearity relation between particles size distribution, RH and also with the physically mixed aerosols. The increase in turbidity coefficient β with RH signifies decrease in visibility with increase in RH.

Table 12 the result of the analysis of equations (8) and (12) using SPSS.

	μ	13.30796	
λ	R^2	γ	ν
0.55	0.95143	0.086552	2.151831
0.65	0.941556	0.074656	1.993519
0.75	0.93378	0.064638	1.860276

By observing the values of R^2, it can be said that the data fitted the equation models very well. Equation (6) shows that the visibility satisfies the inverse power law with (1-RH). The decrease in the magnitude of the humidification factor with wavelength also shows that the visibility increases with the increase in wavelength. Equation (12) shows that the hygroscopic growth has satisfied the inverse power relation also with (1-RH) and the reciprocal of mean exponent of aerosol growth curve. It can also be said that for a fixed value of mean exponent of the aerosol growth curve μ, the humidification factor γ decreases with the increase in wavelength, this also shows that as the particles size decreases, which further signifies that the visibility increased with the increase in wavelength, i.e it satisfies the inverse power law of equation (6). Based on equation (9), the mean exponent of the aerosol size distribution (ν) decrease with the increase in wavelength, which shows that the number of larger particles increase compared to smaller particles and this is due to major coagulation amount caused by the increase in number of fine mode particles and consequently the tiny particles coagulate more than the larger particles as said by [29,32]. It can also be noted from the values of (ν) that the average atmospheric condition of the area is foggy [31].

Table 13 the results of the analysis of skewness and kurtosis using SPSS.

	lnvis00	lnvis50	lnvis70	lnvis80	lnvis90	lnvis95	lnvis98	lnvis99
Skewness	-0.2695	-0.2418	-0.5168	-0.4062	-0.5196	-0.4129	-0.2253	-0.2072
Kurtosis	-0.8820	-0.7605	-0.8824	-1.0516	-0.9402	-0.7530	-1.1492	-1.2656

From Table 13, the behaviors and changes of particles size distribution are displayed in terms of vertical behavior (kurtosis) and horizontal behavior (skewness). From skewness, it can be seen that it is negative all through, this implies that it is negatively skewed and this signifies that the particle distribution is dominated by coarse mode particles. From the kurtosis, it can be observed that it is also negative all through, and this shows that it is platykurtic, and the average vertical size distribution of the particles is below normal size distribution. The fluctuations in the values of the values of skewness and kurtosis maybe due to the nonlinear relation between the particles size distribution with RH and the physically mixed aerosols.

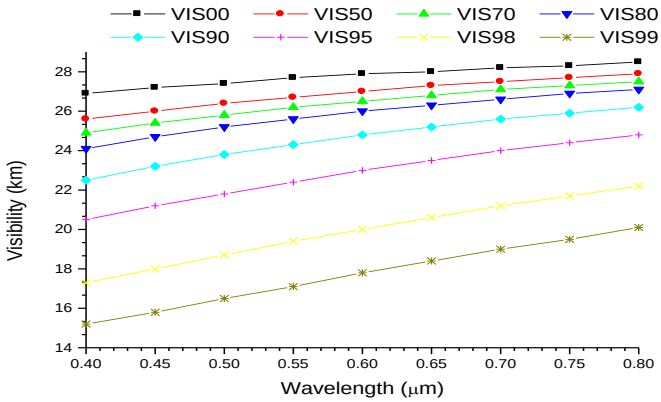

Figure 5 a graph of visibility against wavelength for micn model 5

From figure 5, it can be observed that the visibility increases with the increase in wavelength, and decreases with the increase in relative humidity (RH). It can also be observed that the visibility is lower at shorter wavelengths with maximum and minimum values of about 27.1km and 15.2km respectively. This shows the dominance of coarse mode particles with some traces of fine mode particles. It should also be noted that fine mode particles scatter and absorb more solar radiation than the coarse mode particles [33]. Since from equation (3) the visibility is the inverse of extinction, this implies that the visibility will be lower at shorter wavelengths. The change in visibility is more pronounced from 80%RH to 99%RH.

Table 14 Results of the regression analysis of equations (4) and (5) for visibility using SPSS.

	Linear			Quadratic			
RH	R^2	α	β	R^2	α_1	α_2	β
0%	0.9669	0.0884	0.1270	0.9781	0.0340	-0.0482	0.1286
50%	0.9887	0.1351	0.1279	0.9937	0.0799	-0.0489	0.1296
70%	0.9927	0.1566	0.1291	0.9977	0.0930	-0.0564	0.1311
80%	0.9946	0.1830	0.1303	0.9949	0.1647	-0.0162	0.1309
90%	0.9938	0.2285	0.1337	0.9960	0.1665	-0.0550	0.1357
95%	0.9990	0.2915	0.1402	0.9990	0.2952	0.0032	0.1401
98%	0.9981	0.3835	0.1542	0.9983	0.3545	-0.0257	0.1553
99%	0.9976	0.4259	0.1701	0.9993	0.5275	0.0901	0.1661

Observing the R^2 values from both the linear and quadratic part of Table 14, it can be seen that the data fitted the equation models very well. From the linear part, since α (angstrom exponent) is less than 1, this signifies the dominance of coarse mode particles. The increase of α with RH shows that coarse mode particles are being reduced from the atmosphere more than fine mode particles as a

result of the increase in RH due to coagulation and sedimentation. Considering the quadratic part, it can be seen that α^2 is negative (monomodal distribution of coarse mode particles) all through except at 95% and 99%RH which are positive (bimodal type of distribution with coarse mode particles as dominant and traces of fine mode particles) respectively. The fluctuations of the magnitudes of α^2 with RH shows the non-linearity relation between particles size distribution, RH and also with the physically mixed aerosols. The increase in turbidity coefficient β with RH signifies decrease in visibility with increase in RH.

Table 15 the result of the analysis of equations (8) and (12) using SPSS.

	μ	13.48636	
λ	R^2	γ	ν
0.55	0.950969	0.08569	2.155646
0.65	0.942124	0.074044	1.998584
0.75	0.933491	0.063985	1.862925

By observing the values of R^2, it can be said that the data fitted the equation models very well. Equation (6) shows that the visibility satisfies the inverse power law with (1-RH). The decrease in the magnitude of the humidification factor with wavelength also shows that the visibility increases with the increase in wavelength. Equation (12) shows that the hygroscopic growth has satisfied the inverse power relation also with (1-RH) and the reciprocal of mean exponent of aerosol growth curve. It can also be said that for a fixed value of mean exponent of the aerosol growth curve μ, the humidification factor γ decreases with the increase in wavelength, this also shows that as the particles size decreases, which further signifies that the visibility increased with the increase in wavelength, i.e it satisfies the inverse power law of equation (6). Based on equation (9), the mean exponent of the aerosol size distribution (v) decrease with the increase in wavelength, which shows that the number of larger particles increase compared to smaller particles and this is due to major coagulation amount caused by the increase in number of fine mode particles and consequently the tiny particles coagulate more than the larger particles as said by [29,32]. It can also be noted from the values of (v) that the average atmospheric condition of the area is foggy [31].

Table 16 the results of the analysis of skewness and kurtosis using SPSS.

	lnvis00	lnvis50	lnvis70	lnvis80	lnvis90	lnvis95	lnvis98	lnvis99
Skewness	-0.5567	-0.4323	-0.4681	-0.4062	-0.5196	-0.4129	-0.2557	-0.2434
Kurtosis	-0.6429	-1.0766	-0.5646	-1.0516	-0.9402	-0.7530	-1.0281	-1.0411

From Table 16, the behaviors and changes of particles size distribution are displayed in terms of vertical behavior (kurtosis) and horizontal behavior (skewness). From skewness, it can be seen that it is negative all through, this implies that it is negatively skewed and this signifies that the particle distribution is dominated by coarse mode particles. From the kurtosis, it can be observed that it is also negative all through, and this shows that it is platykurtic, and the average vertical size distribution of the particles is below normal size distribution. The fluctuations in the values of the values of skewness and kurtosis maybe due to the nonlinear relation between the particles size distribution with RH and the physically mixed aerosols.

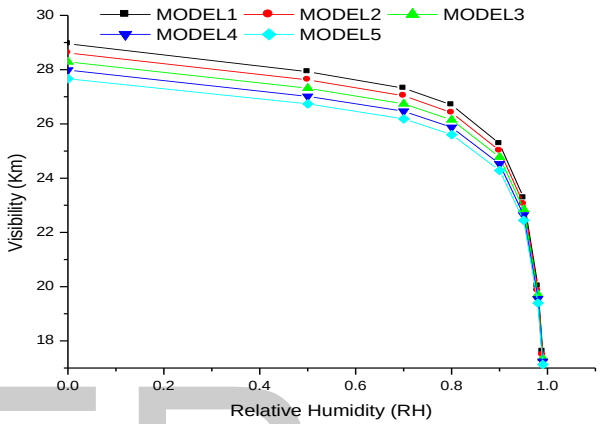

Figure 6 plot of Visibility against Relative Humidity (RH%) at 0.55μm spectral wavelength (green) and varrying MICN concentrartion

It can be observed from fig. 6 that the visibility decrease with the increase in MICN concentrations and also decresease with the increase in RH across the five models.

4 Summary

From the models considered (1-5), it was observed that

I. the (α) angstrom exponent values are less than 1 throughout and decreased with the increase in RHs and aerosols concentrations except for model5.
II. The curvature (α^2) is observed to be both monomodal and bimodal type of distribution at all the RHs, and the magnitude fluctuate across the models.
III. It can be observed that the turbidity coefficient β increase with the increase in RH across all the models, this implies that the visibility decreases with the increase in RH.
IV. Based on the results of the analysis of equations (6), (9), (12) and the plots of visibility against the wavelengths, it can be observed that there is an inverse relation between the humidification factor γ, the mean exponent of the aerosol size distribution v with the particles concentration (i.e as the magnitudes of the humidification factor and the mean exponent of aerosol size distribution increase with the increase in the concentration of the particles and the increase in wavelengths across the models, the visibility decreases

across the models). It can also be observed that as the magnitude of the mean exponent of aerosol growth curve (μ) increase with the increase in particles concentration and the increase of wavelengths across the models, the magnitudes of the humidification factor (γ) and the mean exponent of aerosol size distribution (v) also increase with the increase across the models.

V. It can be observed that there are fluctuations in the magnitude of the skewness and kurtosis across the studied models. This may be due to the nonlinear relationship between the particle size distribution and the physically mixed aerosols with RH.

5.0 Conclusion

So, it can be concluded that, the visibility decreases with the increase in RHs, increase in MICN (particles concentration) and with the increase in wavelengths. Also, the decrease in the magnitude of the values of (α) across the models (except for model 5) and at all RHs implied coarse mode particles are being removed from the atmosphere due to major coagulation and sedimentation. the fluctuations of (α2) as a result of the change in RHs and particle concentrations signifies nonlinear relationship between RHs and the physically mixed aerosols. It can also be concluded that the visibility decreased with the increase in the magnitudes of both the humidification factor (γ) and the mean exponent of aerosol size distribution (v). there is a direct relationship between the mean exponent of aerosol size distribution, the humidification factor and with the mean exponent of aerosol growth curve. Additionally, the fluctuations in the magnitude of skewness and kurtosis also signifies that there is dominance of coarse mode particles with some traces of fine mode particles across the models and that the relationship between the particles size distribution, RHs with the physically mixed aerosols is nonlinear.

References

[1] M. S. Quinby-Hunt, L. L. Erskine, and A. J. Hunt, "Polarized light scattering by aerosols in the marine atmospheric boundary layer," Appl. Opt., vol. 36, no. 21, p. 5168, 1997, doi: 10.1364/ao.36.005168.

[2] E. P. Shettle and R. W. Fenn, "MODELS OF THE ATMOSPHERIC AEROSOLS AND THEIR OPTICAL PROPERTIES.," in AGARD Conf Proc, 1975, no. N 183.

[3] H. Lee, O. V. Kalashnikova, K. Suzuki, A. Braverman, M. J. Garay, and R. A. Kahn, "Climatology of the aerosol optical depth by components from the Multi-angle Imaging SpectroRadiometer (MISR) and chemistry transport models," Atmos. Chem. Phys., 2016, doi: 10.5194/acp-16-6627-2016.

[4] J. H. Seinfeld and J. Wiley, ATMOSPHERIC From Air Pollution to Climate Change SECOND EDITION. 2006.

[5] M. Balarabe, K. Abdullah, and M. Nawawi, "Long-term trend and seasonal variability of horizontal visibility in Nigerian troposphere," Atmosphere (Basel)., vol. 6, no. 10, pp. 1462–1486, 2015, doi: 10.3390/atmos6101462.

[6] O. K. Nwofor, "Rising Dust Aerosol Pollution at Ilorin in the Sub-sahel Inferred from 10-year Aeronet Data : Possible Links to Persisting Drought Conditions," Earth, vol. 2, no. 4, pp. 216–225, 2010.

[7] K. Megahed, "The Impact of Mineral Dust Aerosol Particles on Cloud Formation," 2006.

[8] S. R. Osborne, B. T. Johnson, J. M. Haywood, A. J. Baran, M. A. J. Harrison, and C. L. McConnell, "Physical and optical properties of mineral dust aerosol during the Dust and Biomass-burning Experiment," J. Geophys. Res. Atmos., vol. 113, no. 23, pp. 1–14, 2008, doi: 10.1029/2007JD009551.

[9] H. Maring, D. L. Savoie, M. A. Izaguirre, L. Custals, and J. S. Reid, "Mineral dust aerosol size distribution change during atmospheric transport," J. Geophys. Res. Atmos., vol. 108, no. 19, 2003, doi: 10.1029/2002jd002536.

[10] S. K. Mishra, S. N. Tripathi, S. G. Aggarwal, and A. Arola, "Optical properties of accumulation mode, polluted mineral dust: Effects of particle shape, hematite content and semi-external mixing with carbonaceous species," Tellus, Ser. B Chem. Phys. Meteorol., vol. 64, no. 1, 2012, doi: 10.3402/tellusb.v64i0.18536.

[11] G. T. Wolff, R. J. Countess, P. J. Groblicki, M. A. Ferman, S. H. Cadle, and J. L. Muhlbaier, "Visibility-reducing species in the denver 'brown cloud'-II. Sources and temporal patterns," Atmos. Environ., vol. 15, no. 12, pp. 2485–2502, 1981, doi: 10.1016/0004-6981(81)90064-0.

[12] S. Tiwari, S. Payra, M. Mohan, S. Verma, and D. S. Bisht, "Visibility degradation during foggy period due to anthropogenic urban aerosol at Delhi, India," Atmos. Pollut. Res., vol. 2, no. 1, pp. 116–120, 2011, doi: 10.5094/APR.2011.014.

[13] P. Tsilimigras, "On the applicability of the Roothaan-Bagus procedure," Chem. Phys. Lett., vol. 11, no. 1, pp. 99–100, 1971, doi: 10.1016/0009-2614(71)80541-9.

[14] R. J. Charlson, "current research," vol. 3, no. 10, pp. 913–918, 1969.

[15] and I. schult M. Hess, P. Koepke, "Optical Properties of Aerosols and Clouds: The Software

Package OPAC," pp. 831–844, 1998.

[16] K. K. Moorthy, A. Saha, B. S. N. Prasad, K. Niranjan, D. Jhurry, and P. S. Pillai, "Aerosol optical depths over peninsular India and adjoining oceans during the INDOEX campaigns: Spatial, temporal, and spectral characteristics," J. Geophys. Res. Atmos., vol. 106, no. D22, pp. 28539–28554, 2001, doi: 10.1029/2001JD900169.

[17] S. Singh, S. Nath, R. Kohli, and R. Singh, "Aerosols over Delhi during pre-monsoon months : Characteristics and effects on surface radiation forcing," vol. 32, pp. 4–7, 2005, doi: 10.1029/2005GL023062.

[18] E. L. Koschmieder, "Symmetric Circulations of Planetary Atmospheres," Adv. Geophys., vol. 20, no. C, pp. 131–181, 1978, doi: 10.1016/S0065-2687(08)60323-4.

[19] M. D. and D. M. B. King, "a method for inferring total ozone content from spectral variation of total optical depth obtained with solar radiometer." 1976.

[20] B. I. Tijjani, F. Sha'aibu, and A. Aliyu, "The Effect of Relative Humidity on Maritime Tropical Aerosols," Open J. Appl. Sci., vol. 04, no. 06, pp. 299–322, 2014, doi: 10.4236/ojapps.2014.46029.

[21] B. I. Tijjani, F. Sha'aibu, and A. Aliyu, "The Effect of Relative Humidity on Maritime Polluted Aerosols," Open J. Appl. Sci., vol. 04, no. 06, pp. 299–322, 2014, doi: 10.4236/ojapps.2014.46029.

[22] N. T. O'Neill, O. Dubovik, and T. F. Eck, "Modified Ångström exponent for the characterization of submicrometer aerosols," Appl. Opt., vol. 40, no. 15, p. 2368, 2001, doi: 10.1364/ao.40.002368.

[23] N. T. O'Neill, T. F. Eck, A. Smirnov, B. N. Holben, and S. Thulasiraman, "Spectral discrimination of coarse and fine mode optical depth," J. Geophys. Res. D Atmos., vol. 108, no. 17, pp. 1–15, 2003, doi: 10.1029/2002jd002975.

[24] J. Kaufman, "Aerosol Optical Thickness and Atmospheric Path Radiance," vol. 98, pp. 2677–2692, 1993.

[25] T. F. Eck, B. N. Holben, A. Smirnov, I. Slutsker, J. M. Lobert, and V. Ramanathan, "Column-integrated aerosol optical properties over the Maidives during the northeast," vol. 106, 2001.

[26] J. S. Reid, A. Smirnov, N. T. O. Neill, I. Slutsker, and S. Kinne, "In / X," vol. 104, no. 1, 1999.

[27] T. F. Eck et al., "Characterization of the optical properties of biomass burning aerosols in Zambia during the 1997 ZIBBEE field campaign," vol. 106, pp. 3425–3448, 2001.

[28] F. Kasten, "Visibility forecast in the phase of pre-condensation," Tellus, vol. 21, no. 5, pp. 631–635, Jan. 1969, doi: 10.3402/tellusa.v21i5.10112.

[29] B. I. Tijjani, "The Effect of Soot and Water Soluble on the Hygroscopicity of Urban Aerosols," vol. 26, pp. 52–73, 2013, [Online]. Available: www.iiste.org.

[30] P. K. Quinn et al., "Impact of particulate organic matter o`n the relative humidity dependence of light scattering: A simplified parameterization," Geophys. Res. Lett., vol. 32, no. 22, pp. 1–4, 2005, doi: 10.1029/2005GL024322.

[31] Junge et. al., "Chapter 2 Physical and Optical properties of aerosols," no. 1, 1958.

[32] S. Sjogren, M. Gysel, E. Weingartner, U. Baltensperger, M. J. Cubison, and H. Coe, "Hygroscopic growth and water uptake kinetics of two-phase aerosol particles consisting of ammonium sulfate , adipic and humic acid mixtures," vol. 38, pp. 157–171, 2007, doi: 10.1016/j.jaerosci.2006.11.005.

[33] E. Swietlicki et al., "Hygroscopic properties of submicrometer atmospheric aerosol particles measured with H-TDMA instruments in various environments - A review," Tellus, Ser. B Chem. Phys. Meteorol., vol. 60 B, no. 3, pp. 432–469, 2008, doi: 10.1111/j.1600-0889.2008.00350.x.

[34] R. Lang and N. X. Xanh, "Smoluchowski's theory of coagulation in colloids holds rigorously in the Boltzmann-Grad-limit," Zeitschrift für Wahrscheinlichkeitstheorie und Verwandte Gebiete, vol. 54, no. 3, pp. 227–280, 1980, doi: 10.1007/BF00534345.